Intramolecular Cyclization Dominating Homopolymerization of Multivinyl Monomers toward Single-Chain Cyclized/Knotted Polymeric Nanoparticles

ARTICLE *in* MACROMOLECULES · SEPTEMBER 2015

Impact Factor: 5.8 · DOI: 10.1021/acs.macromol.5b01549

Macromolecules

Article

pubs.acs.org/Macromolecules

Intramolecular Cyclization Dominating Homopolymerization of Multivinyl Monomers toward Single-Chain Cyclized/Knotted Polymeric Nanoparticles

Yongsheng Gao,[†] Dezhong Zhou,[†] Tianyu Zhao,[†] Xuan Wei,[†] Sean McMahon,[†] Jonathan O'Keeffe Ahern,[†] Wei Wang,[†,¶] Udo Greiser,[†] Brian J. Rodriguez,[‡,§] and Wenxin Wang*[,†,¶]

[†]Charles Institute of Dermatology, School of Medicine and Medical Science, [‡]School of Physics, and [§]Conway Institute of Biomolecular and Biomedical Research, University College Dublin, Belfield, Dublin 4, Ireland

[¶]School of Materials Science and Engineering, Tianjin University, Tianjin 300072, China

Supporting Information

ABSTRACT: Polymerization of multifunctional monomers could produce polymers with different functionalities and novel macromolecular architectures. However, the ability to control the homopolymerization of multivinyl monomers (MVMs) has always been a challenge. Here we demonstrate that the homopolymerization of acrylate based MVMs can be kinetically controlled via Cu^0-mediated controlled/living radical polymerization in the presence of additional Cu^{II}, which enables the efficient promotion of intramolecular cyclization and suppression of intermolecular cross-linking. The gelation is effectively delayed over ca. 40% monomer conversion in the concentrated polymerization system ([M] = 40.9 wt %), which is far higher than the Flory−Stockmayer theory predicts. Moreover, closer inspection of the synthesized polymers reveals that single-chain cyclized/knotted polymeric nanoparticles (SCKNPs) are formed due to the nature of one-pot *in situ* intramolecular reaction and self-cyclization of the propagating polymer chains. This facile method opens a new avenue to the design and synthesis of a broad range of novel single-chain cyclized/knotted polymeric materials.

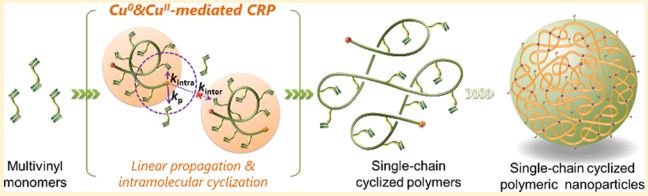

INTRODUCTION

Polymerizations of multifunctional monomers are of great importance to polymer chemists, given that the resulting products should, in principle, contain multiple functional groups and form novel macromolecular architectures by either the involvement of multiple reactive groups during the polymerization process or the postmodifications.[1,2] Despite the increased sophistication in the design of the controlled polymerization techniques, the main challenge associated with this process is the use of widely available multifunctional monomers in a convenient, efficient, and environmentally friendly manner to yield the desired topological structure. For instance, the polymerization of multivinyl monomers (MVMs)—one kind of the most heavily used monomers—would inevitably lead to gelation even at low monomer conversion owning to the presence of significant intermolecular cross-linking reactions according to the classical Flory−Stockmayer theory (F−S theory).[3−5] This prevents the formation of controlled macromolecular structures and high monomer conversion rate, which have been verified experimentally numerous times.[6,7]

There have been continued efforts to control the polymerization process and delay the gelling point for the polymerization of MVMs. Sherrington and co-workers[8−10] introduced a large amount of chain transfer agents into the conventional radical copolymerization of monovinyl monomers and MVMs to inhibit cross-linking and got high monomer conversion. Recently, the evolution of controlled/living radical polymerization (CRP) has also contributed to this field. The CRP of monovinyl monomers and small amounts of MVMs via nitroxide-controlled free radical polymerization (NMP),[11,12] atom transfer radical polymerization (ATRP),[13−15] and reversible addition−fragmentation chain transfer polymerization (RAFT)[16−18] have been utilized to delay the gelling point and attempt to synthesize a soluble polymers with high monomer conversion. Nevertheless, most results indicated that the intermolecular cross-linking degree at the gelling point was still in close alignment with the F−S theory,[11−14,18] while others had a slight discrepancy from F−S theory were attributed to the existence of partial intramolecular cyclization.[15−17] Compared to the copolymerization of monovinyl monomers and MVMs, the controlled homopolymerization of MVMs appears significantly more challenging, given that each MVM is a potential cross-linker, and hence there are much more "cross-linkers" in the homopolymerization reaction compared to the copolymerization system. Unsurprisingly, most published results indicate that gelation occurred at extremely low monomer conversions (<10%) in the homo-

Received: July 13, 2015
Revised: August 25, 2015
Published: September 23, 2015

DOI: 10.1021/acs.macromol.5b01549
Macromolecules 2015, 48, 6882−6889

polymerization of MVMs.[19−22] Those that obtained soluble polymers are attributed to the highly diluted reaction conditions along with poor structural control of the result polymers.[23]

Despite various topologies of synthetic polymers exist including linear, branched, hyperbranched, star, brushed, and cyclic, polymers composed of cyclic units (macrocyclic,[24−27] multicyclic,[28−30] knotted cyclic,[31−33] and folded cyclic[34−36]) are of significant interest due to their compact architectures and resulting unique properties. These properties include a high density, low intrinsic viscosity, low translational friction coefficients, high glass transition temperatures,[37] great elasticity of the formed network,[38] reduced cytotoxicity, and increased circulation time for drug and gene delivery applications.[39,40]

However, efficient and practical syntheses of the cyclic architectures are among the most difficult tasks for polymer chemists, as the polymer chains must react with themselves prior to reacting with other chains.[30,41,42] Thus far, to achieve such intramolecular reactions rather than intermolecular reactions, it is necessary to work under extreme diluted conditions,[42,43] or in one-dimensional channels,[44] or, alternatively, to perform the cyclopolymerization of the designed monomers which are in favor of the intramolecular reaction through an energy lowering effect and steric control.[45,46] Developing an effective approach to regulate the occurrence of the intermolecular and intramolecular reactions should, in principle, open new avenues to efficiently design and synthesize polymers containing cyclic structures.

Interestingly, a deactivation enhanced ATRP (DE-ATRP) method was reported previously to control the homopolymerization of MVMs.[47−54] Under this kinetically controlled strategy, the DE-ATRP approach has shown that it is possible to control both the gelling point and the macromolecular architecture within the homopolymerization of MVMs without the need for a diluted reaction condition. This approach efficiently delayed the gelling point up to ca. 50% monomer conversion in concentrated conditions. Moreover, two types of polymeric architectures—novel three-dimensional self-knotted[48,49,52,53] and hyperbranched[50,51,54]—were formed due to the manipulation of intramolecular and intermolecular cross-linking. Despite some drawbacks associated with this technique, namely the required high copper concentrations, these works have opened the door for the design and control of various polymer architectures from the homopolymerization of MVMs.

As a result of extensive studies utilizing copper-based CRP reactions, numerous techniques have been developed to provide a better control over the polymerization behaviors and final polymer structure but with a lower the catalyst concentration, including activators regenerated by electron transfer (ARGET) ATRP,[55] initiators for continuous activator regeneration (ICAR) ATRP,[56] electrochemically mediated ATRP,[57] photochemically mediated ATRP,[58,59] and Cu^0-mediated CRP.[60]

Upon consideration relating to the manipulation of deactivation, attention was drawn to the Cu^0-mediated CRP technique (also known as single electron transfer living radical polymerization (SET-LRP) or supplemental activator and a reducing agent (SARA) ATRP),[60−64] due to its simplicity, mild conditions, tolerance to air, high livingness, and relatively fast polymerization for acrylate-based monomers. Of note, the application of a kinetically controlled strategy for Cu^0-mediated CRP is facilitated by two inherent features: multiple roles of copper species and heterogeneity derived from the presence of metallic copper in the form of a wire or powder, allowing only the surface of Cu^0 to be available for reaction. Despite these advantages, to the best of our knowledge, the Cu^0-mediated CRP has not been employed to polymerize MVMs thus far.

In this paper, the aim was to apply the kinetically controlled concept to Cu^0-mediated CRP to perform the homopolymerization of commercially available acrylate-based MVMs: tetra(ethylene glycol) diacrylate (TEGDA) and bis(2-acryloyl)-oxyethyl disulfide (DSDA). A small amount of Cu^{II} together with ligand *N*,*N*,*N*′,*N*′,*N*″-pentamethyldiethylenetriamine (PMDETA) were added at the beginning of Cu^0-mediated CRP (hereafter termed Cu^0&Cu^{II}-mediated CRP) to enhance the deactivation and therefore kinetically control the polymerization. The addition of Cu^{II} is critical to obtain a well-controlled polymerization, enabling the delay of the gelling point and control of the macromolecular architecture through regulating the occurrence of chain propagation, intramolecular cyclization, and intermolecular cross-linking. More importantly, closer inspection of the newly synthesized polymers revealed that novel single-chain cyclized/knotted polymeric nanoparticles (SCKNPs) were formed due to the nature of the one-pot *in situ* intramolecular reaction and self-cyclization of the propagating polymer chains. This SCKNP should be an ideal candidate as, for instance, efficient cargo carriers due to the existence of in-chain cyclic units.

RESULTS AND DISCUSSION

Controlled Homopolymerization of TEGDA. Motivated by previously reported DE-ATRP, the initial aim was to apply the deactivation enhanced concept to SET-LRP to kinetically control the homopolymerization of MVMs through the addition of Cu^{II} at the start of the polymerization. However, the mechanism behind this system is far more complicated than a presumed deactivation enhanced SET-LRP. Indeed, the exact mechanism behind the Cu^0-mediated CRP is still under debate, with differing views as to the roles of differing copper valences. Put simply, Matyjaszewski and co-workers claimed that the role of Cu^0 was a supplemental activator and a reducing agent (SARA).[61−66] In contrast, SET-LRP, proposed by Percec and co-workers,[60,67,68] emphasized that the initiators were mainly catalyzed by Cu^0 to generate a free radical and Cu^I, followed by the spontaneous disproportionation into Cu^0 and Cu^{II}. Of note, a polymerization of methyl acrylate using Cu^0-mediated polymerization with PMDETA as a ligand in DMSO was found to be poorly controlled. However, the polymerization became well controlled with the addition of a small amount of Cu^{II} at the beginning of the reaction.[69] Nevertheless, utilizing the advantages of Cu^0-mediated CRP as mentioned previously, this Cu^0&Cu^{II} -mediated CRP provides an excellent platform to kinetically control the homopolymerization of MVMs.

The key to a well-controlled homopolymerization of MVMs is to regulate the occurrence of chain propagation, intramolecular cyclization, and intermolecular cross-linking, which necessitates small instantaneous kinetic chain length, i.e., growth boundary, confining the possible number of vinyl groups reacted with the propagation center during the active lifetime. This hypothesis, which has been confirmed by the comparison between conventional free radical polymerization (FRP) and DE-ATRP,[48,50] can be further confirmed by the comparison between Cu^0-mediated polymerization and Cu^0&Cu^{II}-mediated CRP of TEGDA. The reaction conditions and results of the homopolymerization of TEGDA are detailed in Table 1 and Figure 1. Similarly to the FRP, the Cu^0-mediated

DOI: 10.1021/acs.macromol.5b01549
Macromolecules 2015, 48, 6882−6889

Table 1. Reaction Results for the Homopolymerization of TEGDA[a]

	catalyst[b]	time (h)	$M_{w,RI}$[c] (kDa)	$Đ_{RI}$[c]	$M_{w,TRI}$[d] (kDa)	$Đ_{TRI}$[d]	α[d]	monomer conv[e] (%)	pendent vinyl conv[f] (%)
1	Cu^0	0.1	868.1	2.35				2.38	3.6
2	Cu^0&Cu^{II}	1	3.3	1.21	5.9	1.21	0.33	8.3	28.3
3		3	5.0	1.23	8.2	1.26	0.29	16.0	30.7
4		6	8.7	1.39	14.2	1.58	0.29	27.1	34.1
5		8	12.8	1.70	26.6	2.04	0.31	32.5	37.0
6		12	48.8	2.83	179.1	4.44	0.36	40.4	38.4

[a]Reaction condition: [M]:[I]:[L] = 100:1:0.4, [M] = 1.50 M; M = TEGDA, I = ethyl α-bromoisobutyrate (EBriB), L = PMDETA, solvent = DMSO, T = 25 °C. [b]Cu^0 = pretreated Cu(0) wire (l = 5 cm, d = 1 mm), Cu^{II} = $CuBr_2$ (0.2 equiv). [c]$M_{w,RI}$ and $Đ_{RI}$ were characterized using gel permeation chromatography (GPC) with an RI detector. [d]$M_{w,TRI}$, $Đ_{TRI}$, and Mark–Houwink parameter (α) were characterized using GPC with triple detectors (RI, viscometer, and LS). [e]Monomer conversion was calculated by the integration of peaks in the GPC-RI trace. [f]Pendent vinyl conversion were calculated by ^{1}H NMR (see Supporting Information).

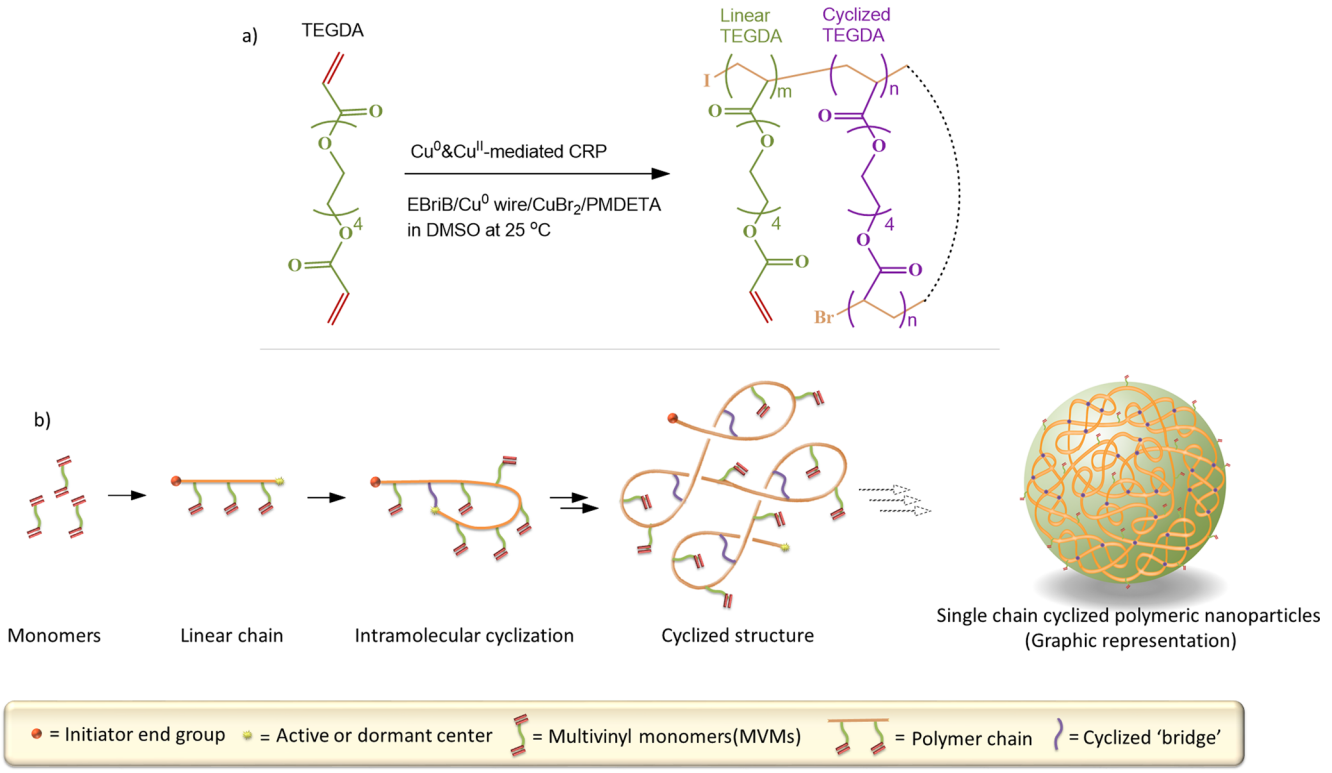

Figure 1. (a) Homopolymerization of TEGDA via Cu^0&Cu^{II}-mediated CRP in DMSO with the ratio of reagents: $[TEGDA]_0/[EBriB]_0/[CuBr_2]_0/[PMDETA]_0$ = 100:1:0.2:0.4, $[TEGDA]_0$ = 1.50 M at 25 °C, in the presence of pretreated Cu(0) wire (l = 5 cm, d = 1 mm). (b) Illustration of the formation process of the single chain cyclized/knotted structure and the final single chain cyclized/knotted polymeric nanoparticles polymers with a potential Celtic knotted structure via Cu^0&Cu^{II}-mediated CRP of TEGDA. The intramolecular cyclization is promoted due to the small kinetic chain length and the high local vinyl concentration near the active center. The graph depicts the way that the single growing chain links to itself, although the final structure is not symmetrical or ordered as shown in the above Celtic knotted structures.

homopolymerization of TEGDA led to a rapid gelation at an extremely low yield (about 3%) with high molecular weight (M_w) and polydispersity ($Đ$) within 0.1 h (Table 1, entry 1), which is in agreement with the prediction of F–S theory. However, there was a significant change in polymerization behavior after the addition of Cu^{II} to this Cu^0-mediated TEGDA homopolymerization system (see entries 2–6 in Table 1 and Figure 2a,b). A substantial delay in gelation point was achieved under a concentrated reaction condition ([TEGDA] = 1.5 M or 40.9 wt %), with gelation occurring after 12 h with a monomer conversion up to 40.4%, which contradicts the established understanding for MVMs polymerization as this yield is significantly greater the F–S theory predicts. Nevertheless, this polymerization process strongly supports the formation of single-chain nanoparticles.

First, monitored by gel permeation chromatography (GPC) at regular time intervals, the polymerization shows two phases (Figure 2a). Stage 1 (<ca. 27% monomer conversion) showed a direct linear relationship between increasing molecular weight and monomer conversion. The molecular weight correlated with the theoretical molecular weight calculated based on the accumulated molecular weight of monomers with one reacted vinyl group ($M_{w,th}$ = [M]/[I] × FW). The $Đ$ during stage 1 remained low ($Đ$ < 1.5) with unimodal GPC peaks. Taking these factors into consideration, we concluded that the polymer chains had a linear growth without intermolecular reactions during this initial stage. Therefore, the primary polymer chains are monodispersed without the combination of multiple chains. This peculiar process greatly differed from that of the Cu^0-mediated polymerization of MVMs and hyperbranched

DOI: 10.1021/acs.macromol.5b01549
Macromolecules 2015, 48, 6882–6889

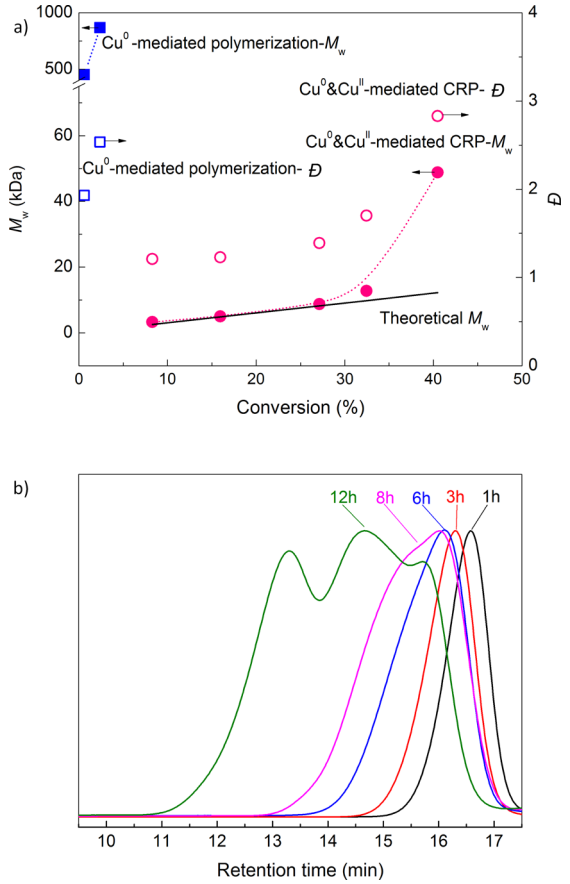

Figure 2. Dependence of the molecular weight (M_w) and polydispersity index ($Đ$) on the monomer conversion for the polymers formed by Cu^0-mediated CRP and Cu^0&Cu^{II}-mediated CRP of TEGDA (a). Time dependence of the composition of the polymerization mixtures monitored by GPC with RI detector for the Cu^0&Cu^{II}-mediated CRP of TEGDA (b).

polymerization systems,[70] in which the drastic combination of primary chains resulted in a rapid rise in molecular weight, along with a significant deviation from the theoretical predictions. At stage 2 of the polymerization, when the polymer concentration exceeded the critical overlap concentration,[71] the polymer chains inevitably began to combine, indicated by a dramatic increase in molecular weight. Moreover, molecular weights achieved were substantially higher than the theoretical molecular weight, accompanied by a $Đ$ value far greater than 1.5 with multimodal GPC peaks.

Furthermore, the conversion of pendent vinyl groups in the samples taken from the linear growth stage is abnormally high (Figure S1 and eq S2). In detail, ca. 15−20% of pendent vinyl groups (see Table 1) were reacted during this linear growth stage even at the onset of the reaction with a very low yield (<5%). This unexpected vinyl consumption is in sharp contrast to the current understanding of the cross-linker role of the divinyl monomers in copolymerization systems,[11−18] which provides evidence for the dominance of intramolecular cyclization occurring during the linear growth process. Specifically, the pendent vinyl groups were consumed intramolecularly and were added into their own backbones to form a self-knotted polymer chain architecture. These structured polymers feature a more compact spherical conformation than their linear counterparts, which is verified by larger $M_{w,TRI}$ compared with $M_{w,RI}$ and smaller Mark−Houwink exponent α (around 0.3, a typical "hard sphere" model). The intramolecular cyclization leads to the consumption of the pendent vinyls without contributing to the increase in molecular weight, which is consistent with the aforementioned agreement between $M_{w,GPC}$ and $M_{w,th}$. Notably, under our experimental conditions, Cu^0&Cu^{II}-mediated CRP can delay the intermolecular cross-linking up to roughly 27% conversion, leading to formation of single-chain nanoparticles with 34.1% pendent vinyl conversion (Table 1, entry 4). Hence, approximately one-third of the pendent vinyl groups are cyclized with their own backbones.

Structural Confirmation of Single Chain Cyclized/Knotted Polymeric Nanoparticles. To further confirm the size, morphology, and constituted structure of these SCKNPs, atomic force microscopy (AFM) and dynamic light scattering (DLS) were employed along with chemical degradation tests.

The purified polymers taken out at 6 h (entry 4, Table 1) with a low $Đ$ value of 1.39 and high pendent vinyl conversion of 34.1% were selected as the optimized SCKNPs to perform the AFM and DLS characterization. Figure 3a displays the topography of SCKNPs imaged in air after drop-casting 25 μL of a dilute SCKNPs acetone solution (0.01 wt %) onto freshly cleaved highly oriented pyrolytic graphite (HOPG). The image shows distinct nanoparticles revealing the morphology of

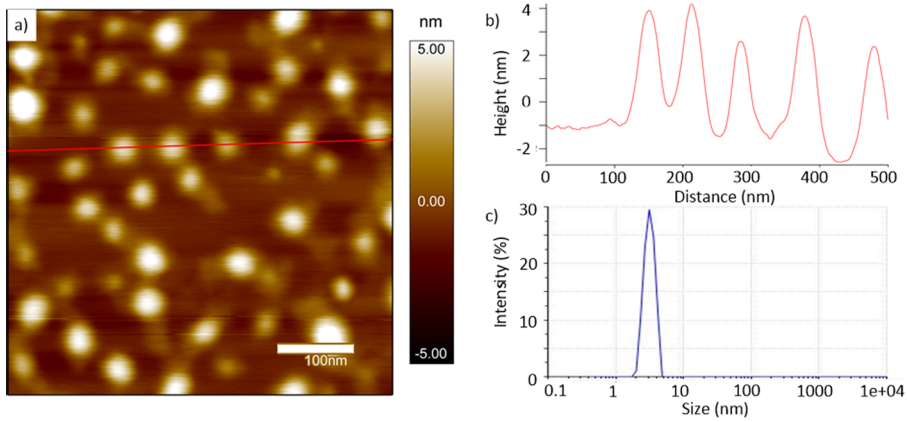

Figure 3. (a) AFM (0.5 × 0.5 μm) topography image of nanoparticles casted on a freshly cleaved highly oriented pyrolytic graphite (HOPG) surface recorded in amplitude modulation mode in air. (b) Height profile across the red line of the AFM image in (a). (c) DLS size distribution of the nanoparticles in (a).

DOI: 10.1021/acs.macromol.5b01549
Macromolecules 2015, 48, 6882−6889

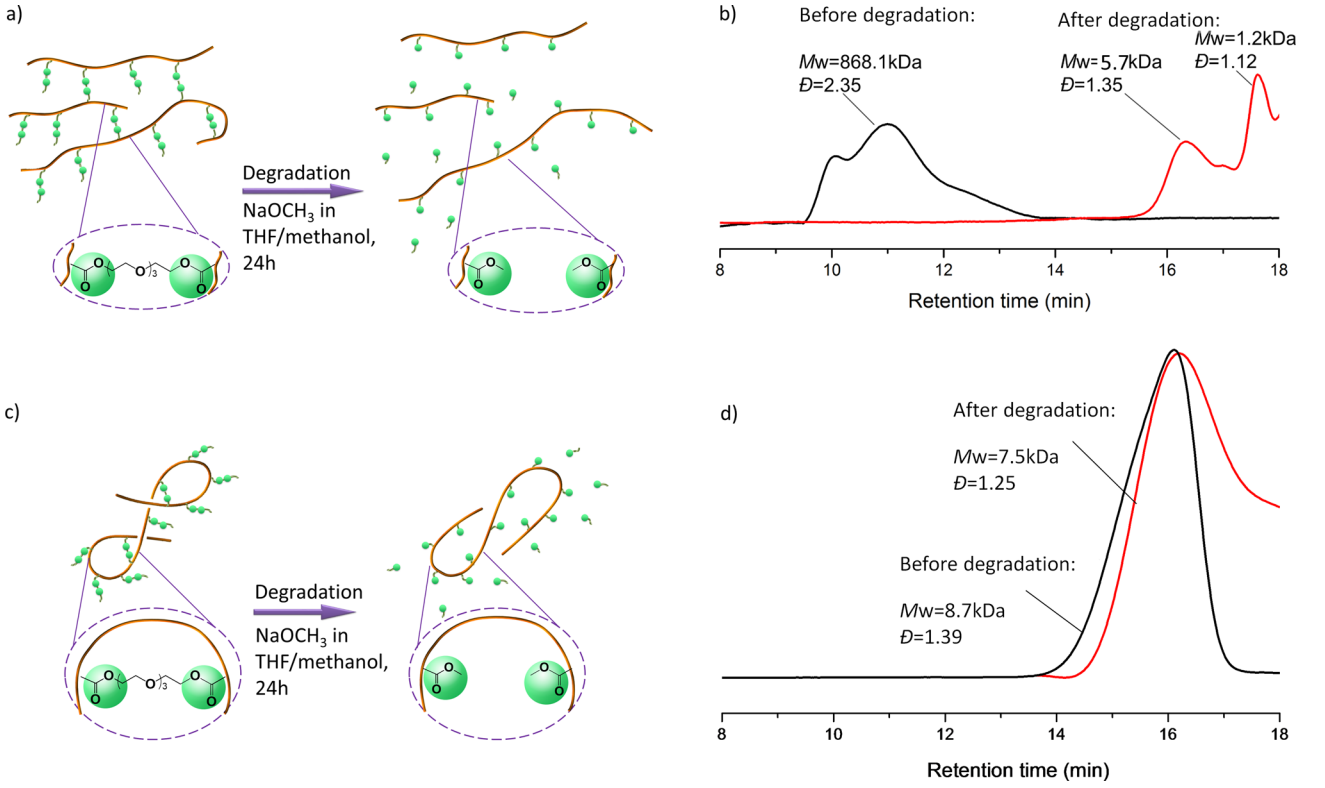

Figure 4. (a, b) Schematic representation and degradation profiles of the polyTEGDA synthesized by Cu^0-mediated polymerization. (c, d) Schematic representation and degradation profiles of the polyTEGDA synthesized by Cu^0&Cu^{II}-mediated CRP. The degradation of polyTEGDA occurs upon cleavage of the ester groups using sodium methoxide in THF/methanol. The GPC traces before and after degradation provides evidence for the "single-chain cyclized/knotted" structure because, unlike the significant decrease in M_w of polymers synthesized by Cu^0-mediated polymerization (b), the M_w only slightly decreased after cleavage from 8.7 to 7.5 kDa for the polymers synthesized by Cu^0&Cu^{II}-mediated CRP (d).

the isolated SCKNPs and also some larger aggregates inevitably formed due to dewetting effects during the casting process.[72] The height profile across the red line in Figure 3b shows that the height of SCKNPs is around 4.4 ± 1.3 nm, which is in agreement with the DLS test result (d_H = 3.5 ± 0.4 nm) as shown in Figure 3c. The much larger width of the nanoparticles can be caused by AFM tip broadening, as has been observed in other studies of polymer nanoparticles.[72] Closer inspection of the interior knotted architecture of the single chain may be hindered by ambient operation and weak polymer−substrate interactions.

Unlike biomacromolecules or polyelectrolytes, imaging neutral synthetic polymer chains of a small size (ranging from a few to several hundred nanometers) remains a challenge to be directly visualized by AFM. Such polymers often appear as compact globules since the polymer chains are softer than biomacromolecules and have weaker interactions with substrates compared with polyelectrolytes.[31] Regardless, the AFM analysis shown here supports the features of the isolated nanoparticles.

To study the single-chain cyclized character of the nanoparticles, the SCKNPs were subjected to chemical degradation under the conditions reported by Hawker et al.[73] The ester groups in the TEGDA molecules can be cleaved by sodium methoxide in a mixture of THF/methanol via an interesterification mechanism. This cleavage enabled us to observe the degradation profile and the constituent primary chains of this cleavable polymer and thereby deduce its structure. For instance, the branched polymer in which the pendent vinyl groups are consumed mainly by the intermolecular cross-link between primary chains with small molecular weight will separate into smaller fragments with a significant decrease in the molecular weight after the breaking of the ester linkages, which has been confirmed by Armes and co-workers[17,74] and our group.[50] On the contrary, the pendent vinyl groups from single-chain cyclized/knotted polymeric nanoparticles are reacted with their own carbon backbone (intramolecular cyclization reaction) to form the multiple "loops" subunits. Hence, we can envisage that a single-chain cyclized/knotted polymer chain will untie to a single linear chain via the breakage of every loop if the ester linkages are cleaved. Significantly, it was shown that the ester groups were completely cleaved according to NMR results (Figure S2), and the molecular weight of SCKNPs decreased from 8.7 to 7.5 kDa (Figure 4), confirming that the degradation is the transfer from a single-chain cyclized/knotted polymer chain to a single linear polymer chain. It should be noted that the slight decrease in molecular weight is due to the removal of parts of the pendent chains after degradation. In contrast, the polymers obtained via Cu^0-mediated polymerization of TEGDA having a high molecular weight and $Đ$ with a low branch ratio were degraded into smaller fragments with a significant decrease in molecular weight, as shown in Figure 4.

Similarly, chemical degradation of other cleavable polymers from the Cu^0&Cu^{II}-mediated CRP of degradable disulfide diacrylate (DSDA) monomers was performed. The disulfide bond in the DSDA molecules can be cleaved by reducing agents, such as tributylphosphine, which are commonly used to prove the polymer structures.[17,50,74] The homopolymerization of DSDA via Cu^0&Cu^{II}-mediated CRP was monitored by GPC

DOI: 10.1021/acs.macromol.5b01549
Macromolecules 2015, 48, 6882−6889

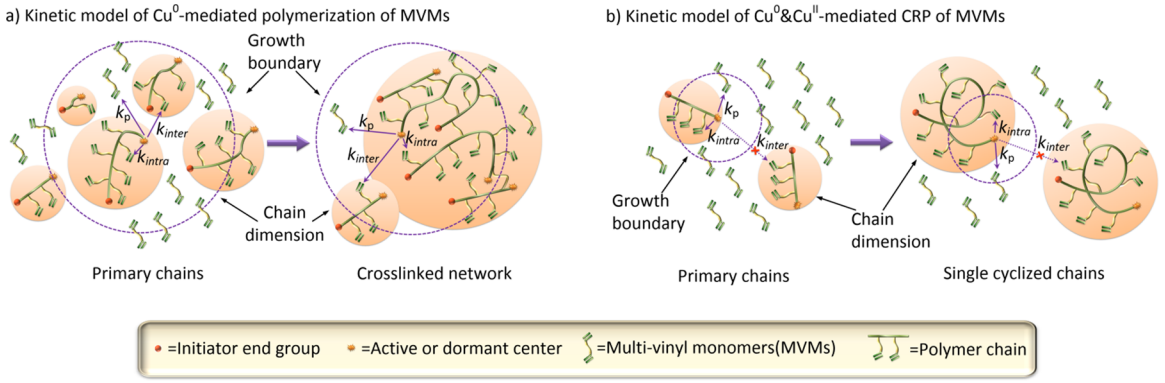

Figure 5. (a) Kinetic model of Cu^0-mediated polymerization of MVMs. (b) Kinetic model of Cu^0&Cu^{II}-mediated polymerization of MVMs. The kinetic model based on three parameters: the growth boundary (dotted circle), chain dimension (shaded part), and chain concentration. The growth boundary shrinks greatly after the incorporation of Cu^{II} compared with Cu^0-mediated polymerization. The smaller growth boundary confines that a smaller number of vinyl groups can react within its active lifetime during the propagation process and, moreover, limits that only the vinyl groups close to the propagation center can be targeted. Therefore, the chain propagation and intramolecular cyclization are promoted, and the intermolecular reaction is suppressed during the early stage in Cu^0&Cu^{II}-mediated CRP because the dimension and concentration of the polymer chains are insufficient to allow overlap.

and showed a similar polymerization profile to that of TEGDA (Figures S3–S5). A two-stage chain growth process also occurred, and samples taken from the early stage had a high pendent vinyl conversion of 19.84% with a low conversion of 12.3%, consistent with the polymerization of TEGDA. The random polyDSDA polymer after degradation exhibited high molecular weight, $Đ$, low branching ratio, and degradation into smaller fragments, evident from the significant decrease in molecular weight as shown in Figure 4. The molecular weight of DSDA-SCKNPs decreased from 4.1 to 2.5 kDa (Figure S6), confirming that the degradation results in the transfer from a single-chain cyclized/knotted polymer chain to a single linear polymer chain. The difference between these two degradation profiles is derived from the different polymer architectures formed via these two different techniques. Together, all of these results provide extensive and conclusive evidence that single-chain nanoparticles were formed from the Cu^0&Cu^{II}-mediated CRP.

Discussion about the Formation Mechanism. During the Cu^0-mediated CRP of monovinyl monomers, the Cu^0 and Cu^I/L are both potentially involved in the activated process and together with the deactivator (Cu^{II}/L) form the reversible activation–deactivation equilibrium to control the development of the three main reactions, i.e., activation, deactivation, and propagation.[60−67] However, another two reactions, i.e., intermolecular cross-linking and intramolecular cyclization, occur when this technique is employed into the homopolymerization of MVMs. As shown in Figure 5, the intermolecular cross-linking and the intramolecular cyclization are competitors of the chain propagation. Control of the competition and occurrence of these three reactions is critical for the preparation of desired polymer structures.

In order to further understand the formation of the single-chain nanoparticles, a kinetic model for homopolymerization of MVMs was developed with three parameters: growth boundary (kinetic chain length), chain dimension, and chain concentration. Figure 5 outlines the models for both Cu^0-mediated polymerization and Cu^0&Cu^{II}-mediated CRP of MVMs. Under the conditions where Cu^{II} is the limiting reagent and insufficient quantities are present to deactivate the active centers and to build the reversible equilibrium, the Cu^0-mediated polymerization technique has larger kinetic chain lengths in the initial stage. As such, the growth boundary confining the large number of vinyl groups added to an active center each time could very justifiably be the reason that allows all of these three reactions to occur (Figure 5a). The resulting high DP_n primary polymer chains would combine to form an insoluble gel instantaneously, regardless of chain dimension and concentration, due to the high rate of propagation and intermolecular cross-linking reactions according to the statistical probability, which is in good accordance with the F–S theory. However, the growth boundary is relatively smaller in the Cu^0&Cu^{II}-mediated CRP of MVMs (Figure 5b) because extra Cu^{II} species are added into the reaction system at the beginning. A smaller growth boundary confines only those very few closest vinyl groups to be added into the active center before it is deactivated. Furthermore, at the early stage of the polymerization, the polymer chain dimension is small and the polymer volume concentration is low; thus, the growth boundary of one polymer has a reduced probability to overlap with that of other polymers. Taking into account the small growth boundary, neglected chain overlap, and the aforementioned three reactions, we can conclude that at the early stage chain propagation and intramolecular cyclization were promoted while intermolecular cross-linking was suppressed. This is due to those vinyl groups nearest the active center either belonging to free monomers or are from the same polymer chain containing the active center, and the vinyl groups from other polymer chains are not in the growth boundary. Therefore, a single-chain cyclized/knotted structure was obtained.

Noteworthy, the SCKNPs derived from the MVMs homopolymerization features the one-pot *in situ* intramolecular reaction and self-knotted propagating polymer chains and thereby has a distinct difference from the single-chain polymeric nanoparticles[75−77]—which are made from the post-intramolecular collapse of primary linear polymer chains—based on the preparation method and topology structure. The facile nature of this kinetically controlled homopolymerization of MVMs allows a wide variation in monomer selection and functional group incorporation to synthesize a variety of multifunctional single-chain polymers.

DOI: 10.1021/acs.macromol.5b01549
Macromolecules 2015, 48, 6882–6889

CONCLUSIONS

In summary, we have demonstrated here that Cu^0&Cu^{II}-mediated CRP can be utilized to conduct a kinetically controlled homopolymerization of MVMs. Moreover, by this approach, novel single-chain nanoparticles, i.e., single-chain cyclized/knotted polymers, were formed due to the intramolecular reaction and self-cyclization of the propagating polymer chains. The comparison between the Cu^0-mediated polymerization and the Cu^0&Cu^{II}-mediated CRP revealed that the addition of the deactivator (Cu^{II}) at the beginning of the reaction is critical to control the polymerization process and the formation of this novel polymer structure, as it allows for the regulation of the occurrence of chain propagation, intramolecular cyclization, and intermolecular cross-linking. The well-controlled homopolymerization via Cu^0&Cu^{II}-mediated CRP indicates the highly applicable nature of the kinetically controlled strategy to CRP and also opens a new avenue to design and synthesize a broad range of novel single-chain cyclized/knotted polymeric materials, which will facilitate their application in a variety of fields.

ASSOCIATED CONTENT

Supporting Information

The Supporting Information is available free of charge on the ACS Publications website at DOI: 10.1021/acs.macromol.5b01549.

Experimental procedures, characterization data, and supporting figures (PDF)

AUTHOR INFORMATION

Corresponding Author

*E-mail wenxin.wang@ucd.ie (W.W.).

Notes

The authors declare no competing financial interest.

ACKNOWLEDGMENTS

The Health Research Board (HRB) of Ireland (HRA/2009/121 and HRA/2009/121/R), Science Foundation Ireland Principal Investigator programme (10/IN.1/B2981(T)), Science Foundation Ireland (SFI07/IN1/B931) (funding for AFM used for this work), and University College Dublin (Scholarship for Y.G.) are gratefully acknowledged for funding.

REFERENCES

(1) Gao, H.; Matyjaszewski, K. *Prog. Polym. Sci.* **2009**, *34*, 317−350.
(2) Chen, Q.; Cao, X.; Xu, Y.; An, Z. *Macromol. Rapid Commun.* **2013**, *34*, 1507−1517.
(3) Flory, P. J. *J. Am. Chem. Soc.* **1941**, *63*, 3096−3100.
(4) Stockmayer, W. H. *J. Chem. Phys.* **1943**, *11*, 45.
(5) Stockmayer, W. H. *J. Chem. Phys.* **1944**, *12*, 125.
(6) Landin, D. T.; Macosko, C. W. C. *Macromolecules* **1988**, *21*, 846−851.
(7) Dotson, N. A.; Diekmann, T.; Macosko, C. W.; Tirrell, M. *Macromolecules* **1992**, *25*, 4490−4500.
(8) Costello, P.; Martin, I.; Slark, A.; Sherrington, D.; Titterton, A. *Polymer* **2002**, *43*, 245−254.
(9) O'Brien, N.; McKee, A.; Sherrington, D. C.; Slark, A. T.; Titterton, A. *Polymer* **2000**, *41*, 6027−6031.
(10) Baudry, R.; Sherrington, D. C. *Macromolecules* **2006**, *39*, 1455−1460.
(11) Ide, N.; Fukuda, T. *Macromolecules* **1997**, *30*, 4268−4271.
(12) Ide, N.; Fukuda, T. *Macromolecules* **1999**, *32*, 95−99.
(13) Bannister, I.; Billingham, N. C.; Armes, S. P.; Rannard, S. P.; Findlay, P. *Macromolecules* **2006**, *39*, 7483−7492.
(14) Gao, H.; Min, K.; Matyjaszewski, K. *Macromolecules* **2007**, *40*, 7763−7770.
(15) Gao, H.; Miasnikova, A.; Matyjaszewski, K. *Macromolecules* **2008**, *41*, 7843−7849.
(16) Liu, B.; Kazlauciunas, A.; Guthrie, J. T.; Perrier, S. *Macromolecules* **2005**, *38*, 2131−2136.
(17) Vo, C.-D. D.; Rosselgong, J.; Armes, S. P.; Billingham, N. C. *Macromolecules* **2007**, *40*, 7119−7125.
(18) Rosselgong, J.; Armes, S. P.; Barton, W.; Price, D. *Macromolecules* **2009**, *42*, 5919−5924.
(19) Yu, Q.; Zeng, F.; Zhu, S. *Macromolecules* **2001**, *34*, 1612−1618.
(20) Yu, Q.; Zhang, J.; Cheng, M.; Zhu, S. *Macromol. Chem. Phys.* **2006**, *207*, 287−294.
(21) Yu, Q.; Zhu, Y.; Ding, Y.; Zhu, S. *Macromol. Chem. Phys.* **2008**, *209*, 551−556.
(22) Kannurpatti, A. R.; Lu, S.; Bunker, G. M.; Bowman, C. N. *Macromolecules* **1996**, *29*, 7310−7315.
(23) Mori, H.; Tsukamoto, M. *Polymer* **2011**, *52*, 635−645.
(24) Jia, Z.; Monteiro, M. J. *J. Polym. Sci., Part A: Polym. Chem.* **2012**, *50*, 2085−2097.
(25) Bielawski, C. W.; Benitez, D.; Grubbs, R. H. *Science (Washington, DC, U. S.)* **2002**, *297*, 2041−2044.
(26) Yudin, A. K. *Chem. Sci.* **2015**, *6*, 30−49.
(27) Schlosser, F.; Sung, J.; Kim, P.; Kim, D.; Würthner, F. *Chem. Sci.* **2012**, *3*, 2778.
(28) Honda, S.; Yamamoto, T.; Tezuka, Y. *J. Am. Chem. Soc.* **2010**, *132*, 10251−10253.
(29) Schappacher, M.; Deffieux, A. *Science (Washington, DC, U. S.)* **2008**, *319*, 1512−1515.
(30) Sugai, N.; Heguri, H.; Ohta, K.; Meng, Q.; Yamamoto, T.; Tezuka, Y. *J. Am. Chem. Soc.* **2010**, *132*, 14790−14802.
(31) Schappacher, M.; Deffieux, A. *Angew. Chem., Int. Ed.* **2009**, *48*, 5930−5933.
(32) Saitta, A. M.; Soper, P. D.; Wasserman, E.; Klein, M. L. *Nature* **1999**, *399*, 46−48.
(33) Dasgupta, S.; Wu, J. *Chem. Sci.* **2012**, *3*, 425−432.
(34) Stals, P. J. M.; Gillissen, M. A. J.; Paffen, T. F. E.; De Greef, T. F. A.; Lindner, P.; Meijer, E. W.; Palmans, A. R. A.; Voets, I. K. *Macromolecules* **2014**, *47*, 2947−2954.
(35) Roy, R.; Lutz, J. *J. Am. Chem. Soc.* **2014**, *136*, 12888−12891.
(36) Ouchi, M.; Badi, N.; Lutz, J.-F. J.; Sawamoto, M. *Nat. Chem.* **2011**, *3*, 917−924.
(37) Zhang, K.; Lackey, M. A.; Cui, J.; Tew, G. N. *J. Am. Chem. Soc.* **2011**, *133*, 4140−4148.
(38) Wei, H.; Chu, D. S. H.; Zhao, J.; Pahang, J. A.; Pun, S. H. *ACS Macro Lett.* **2013**, *2*, 1047−1050.
(39) Nasongkla, N.; Chen, B.; Macaraeg, N.; Fox, M. E.; Fréchet, J. M. J.; Szoka, F. C. *J. Am. Chem. Soc.* **2009**, *131*, 3842−3843.
(40) Chen, B.; Jerger, K.; Fréchet, J. M. J.; Szoka, F. C. *J. Controlled Release* **2009**, *140*, 203−209.
(41) Matyjaszewski, K. *Science (Washington, DC, U. S.)* **2011**, *333*, 1104−1105.
(42) Lu, D.; Jia, Z.; Monteiro, M. J. *Polym. Chem.* **2013**, *4*, 2080−2089.
(43) Jacobson, H.; Stockmayer, W. H. *J. Chem. Phys.* **1950**, *18*, 1600.
(44) Uemura, T.; Nakanishi, R.; Kaseda, T.; Uchida, N.; Kitagawa, S. *Macromolecules* **2014**, *47*, 7321−7326.
(45) Butler, G. B.; Angelo, R. J. *J. Am. Chem. Soc.* **1957**, *79*, 3128−3131.
(46) Butler, G. B.; Bergen, G. *J. Polym. Sci., Part A: Polym. Chem.* **2000**, *38*, 3451−3461.
(47) Wang, W.; Zheng, Y.; Roberts, E.; Duxbury, C. J.; Ding, L.; Irvine, D. J.; Howdle, S. M. *Macromolecules* **2007**, *40*, 7184−7194.
(48) Zheng, Y.; Cao, H.; Newland, B.; Dong, Y.; Pandit, A.; Wang, W. *J. Am. Chem. Soc.* **2011**, *133*, 13130−13137.
(49) Newland, B.; Zheng, Y.; Jin, Y.; Abu-Rub, M.; Cao, H.; Wang, W.; Pandit, A. *J. Am. Chem. Soc.* **2012**, *134*, 4782−4789.

DOI: 10.1021/acs.macromol.5b01549
Macromolecules 2015, 48, 6882−6889

(50) Zhao, T.; Zheng, Y.; Poly, J.; Wang, W. *Nat. Commun.* **2013**, *4*, 1873.
(51) Zheng, Y.; Zhao, T.; Newland, B.; Poly, J.; Wang, W. *Chem. Commun. (Cambridge, U. K.)* **2013**, *49*, 10124−10126.
(52) Newland, B.; Abu-Rub, M.; Naughton, M.; Zheng, Y.; Pinoncely, a V; Collin, E.; Dowd, E.; Wang, W.; Pandit, A. *ACS Chem. Neurosci.* **2013**, *4*, 540−546.
(53) Newland, B.; Aied, A.; Pinoncely, A. V.; Zheng, Y.; Zhao, T.; Zhang, H.; Niemeier, R.; Dowd, E.; Pandit, A.; Wang, W. *Nanoscale* **2014**, *6*, 7526−7533.
(54) Zhao, T.; Zhang, H.; Newland, B.; Aied, A.; Zhou, D.; Wang, W. *Angew. Chem., Int. Ed.* **2014**, *53*, 6095−6100.
(55) Jakubowski, W.; Matyjaszewski, K. *Angew. Chem., Int. Ed.* **2006**, *45*, 4482−4486.
(56) Matyjaszewski, K.; Jakubowski, W.; Min, K.; Tang, W.; Huang, J.; Braunecker, W. A.; Tsarevsky, N. V. *Proc. Natl. Acad. Sci. U. S. A.* **2006**, *103*, 15309−15314.
(57) Magenau, A. J. D.; Strandwitz, N. C.; Gennaro, A.; Matyjaszewski, K. *Science (Washington, DC, U. S.)* **2011**, *332*, 81−84.
(58) Treat, N. J.; Sprafke, H.; Kramer, J. W.; Clark, P. G.; Barton, B. E.; Read de Alaniz, J.; Fors, B. P.; Hawker, C. J. *J. Am. Chem. Soc.* **2014**, *136*, 16096−16101.
(59) Konkolewicz, D.; Schröder, K.; Buback, J.; Bernhard, S.; Matyjaszewski, K. *ACS Macro Lett.* **2012**, *1*, 1219−1223.
(60) Rosen, B. M.; Percec, V. *Chem. Rev.* **2009**, *109*, 5069−5119.
(61) Peng, C.-H.; Zhong, M.; Wang, Y.; Kwak, Y.; Zhang, Y.; Zhu, W.; Tonge, M.; Buback, J.; Park, S.; Krys, P.; Konkolewicz, D.; Gennaro, A.; Matyjaszewski, K. *Macromolecules* **2013**, *46*, 3803−3815.
(62) Wang, Y.; Zhong, M.; Zhu, W.; Peng, C.-H.; Zhang, Y.; Konkolewicz, D.; Bortolamei, N.; Isse, A. A.; Gennaro, A.; Matyjaszewski, K. *Macromolecules* **2013**, *46*, 3793−3802.
(63) Konkolewicz, D.; Wang, Y.; Zhong, M.; Krys, P.; Isse, A. A.; Gennaro, A.; Matyjaszewski, K. *Macromolecules* **2013**, *46*, 8749−8772.
(64) Zhong, M.; Wang, Y.; Krys, P.; Konkolewicz, D.; Matyjaszewski, K. *Macromolecules* **2013**, *46*, 3816−3827.
(65) West, A. G.; Hornby, B.; Tom, J.; Ladmiral, V.; Harrisson, S.; Perrier, S. *Macromolecules* **2011**, *44*, 8034−8041.
(66) Zhang, Y.; Wang, Y.; Peng, C.; Zhong, M.; Zhu, W.; Konkolewicz, D.; Matyjaszewski, K. *Macromolecules* **2012**, *45*, 78−86.
(67) Percec, V.; Guliashvili, T.; Ladislaw, J. S.; Wistrand, A.; Stjerndahl, A.; Sienkowska, M. J.; Monteiro, M. J.; Sahoo, S. *J. Am. Chem. Soc.* **2006**, *128*, 14156−14165.
(68) Zhang, N.; Samanta, S. R.; Rosen, B. M.; Percec, V. *Chem. Rev.* **2014**, *114*, 5848−5958.
(69) Gao, Y.; Zhao, T.; Wang, W. *RSC Adv.* **2014**, *4*, 61687−61690.
(70) Müller, A. H. E.; Yan, D.; Wulkow, M. *Macromolecules* **1997**, *30*, 7015−7023.
(71) Li, Y.; Ryan, A. J.; Armes, S. P. *Macromolecules* **2008**, *41*, 5577−5581.
(72) Wong, E. H. H.; Lam, S. J.; Nam, E.; Qiao, G. G. *ACS Macro Lett.* **2014**, *3*, 524−528.
(73) Paulusse, J. M. J.; Amir, R. J.; Evans, R. A.; Hawker, C. J. *J. Am. Chem. Soc.* **2009**, *131*, 9805−9812.
(74) Rosselgong, J.; Armes, S. P.; Barton, W. R. S.; Price, D. *Macromolecules* **2010**, *43*, 2145−2156.
(75) Foster, E. J.; Berda, E. B.; Meijer, E. W. *J. Am. Chem. Soc.* **2009**, *131*, 6964−6966.
(76) Harth, E.; Van Horn, B.; Lee, V. Y.; Germack, D. S.; Gonzales, C. P.; Miller, R. D.; Hawker, C. J. *J. Am. Chem. Soc.* **2002**, *124*, 8653−8660.
(77) Seo, M.; Beck, B. J.; Paulusse, J. M. J.; Hawker, C. J.; Kim, S. Y. *Macromolecules* **2008**, *41*, 6413−6418.

DOI: 10.1021/acs.macromol.5b01549
Macromolecules 2015, 48, 6882−6889